



Improving the Solar Carbothermal Reduction of Magnesia as a Production Process of Metal Fuels

Youssef Berro, Jean Puig, Marianne Balat-Pichelin

► To cite this version:

Youssef Berro, Jean Puig, Marianne Balat-Pichelin. Improving the Solar Carbothermal Reduction of Magnesia as a Production Process of Metal Fuels. International Journal of Mining, Materials, and Metallurgical Engineering, 2021, 7, pp.22. <10.11159/ijmmme.2021.003>. <hal-03622769>

HAL Id: hal-03622769

<https://hal.science/hal-03622769v1>

Submitted on 29 Mar 2022

HAL is a multi-disciplinary open access archive for the deposit and dissemination of scientific research documents, whether they are published or not. The documents may come from teaching and research institutions in France or abroad, or from public or private research centers.

L'archive ouverte pluridisciplinaire **HAL**, est destinée au dépôt et à la diffusion de documents scientifiques de niveau recherche, publiés ou non, émanant des établissements d'enseignement et de recherche français ou étrangers, des laboratoires publics ou privés.



HAL Authorization

Improving the Solar Carbothermal Reduction of Magnesia as a Production Process of Metal Fuels

Youssef Berro, Jean Puig, Marianne Balat-Pichelin

Laboratoire PROcédés, Matériaux et Energie Solaire PROMES-CNRS, UPR 8521

7 rue du four solaire, 66120 Font-Romeu-Odeillo, France

youssef.berro@promes.cnrs.fr ; j.puig@laposte.net ; marianne.balat@promes.cnrs.fr

Abstract - Recent studies focused on the carbothermal reduction of magnesia as a possible production process of metallic Mg powders that can be used as transportation fuels due to their high energetic value, absence of greenhouse gas emissions, and the ability to regenerate them (through reduction/combustion cycles). Herein, we investigated the development of the reduction process, under vacuum, in the Sol@rmet reactor using concentrated solar energy and charcoal reducing agent as sustainable sources. We shown that the reduction is improved by controlling various parameters as the argon flow, the heating rate, the retention time, the type of the collector filter, and the binder used to form the C/MgO pellets. In fact, a circulating swirl flow inside the reactor allows to prevent the condensation of the produced Mg inside the reactor and to purge out the produced CO, thus reducing its partial pressure and accelerating the reaction. Moreover, using a metallic filter has improved the collection of produced Mg powders. Finally, we found that polyvinyl alcohol (PVA) and bentonite binders have a catalytic effect on the reaction with the best Mg yield of around 96%, with 96% Mg purity, reached when the temperature is raised progressively over 22 min and using 5% starch + 5% bentonite binders.

Keywords: metallic fuels, carbothermal reduction, magnesia, concentrated solar energy, high temperature.

© Copyright 2021 Authors - This is an Open Access article published under the Creative Commons Attribution License terms (<http://creativecommons.org/licenses/by/3.0>). Unrestricted use, distribution, and reproduction in any medium are permitted, provided the original work is properly cited.

1. Introduction

Today, the debate continues worldwide considering two related critical issues, the depletion of fossil fuels and the global warming [1]. The interest of using metallic powders as transportation fuels comes from their high energetic value, the absence of greenhouse

emissions during their combustion, and the ability to regenerate them [2]. The prospect of regenerating metallic fuels, through the reduction of their combustion oxide products, using concentrated solar energy comes from the production of sustainable energy-carrying materials through combustion/reduction cycles.

Previous thermodynamic studies proved that the reduction of magnesia can be assisted using carbon reducing agents as the equilibrium temperature is decreased from 3700 to 2130 K [3], [4]. The use of vacuum-assisted solar furnace is advantageous as it reduces the reduction temperature with lower exergy cost [5]. In fact, the onset temperature of the magnesia carbothermal reduction decreases from 1800 to 1300 K as the pressure decreases from P_{atm} to 10 Pa [6]. Xiong *et al.* [7] proved that under low pressure and considerable flow rate, the CO partial pressure is reduced, which limits the gas-solid reaction and promotes the solid-solid MgO-C phase boundary reaction. Further, operating under low vacuum conditions will prevent the possible oxidation (through the backward reaction with CO) of the produced metallic powders during their condensation, which allows to obtain a high purity product [7], [8]. Moreover, a slow preheating will decrease the starting and average temperatures of the reaction, which will necessitate longer reaction times meaning more MgO sintering. Hence, the use of concentrated solar energy is advantageous as high temperatures can be reached rapidly [9], [10].

Early experimental research by Fruehan *et al.* [11] in 1996, proved that coconut charcoal is more reactive than graphite during magnesia reduction as it has a higher surface area (1050 m²/g) allowing a higher contact area with MgO. In addition, they confirmed that

the reaction rate declines as the carbon particle size and the carbon content decrease. In fact, an excess of carbon ($C/MgO = 2$) will improve the reduction yield [11]. Later kinetic studies proved that the reduction rate is faster using charcoal than graphite (thermal gravimetric) [12] or carbon black (solar-driven) [13], and then it follows the same trend. This behavior is attributed to the two-step reaction where, at low temperature, the rate is favored by the MgO -C contact (solid-solid reaction affected by the carbon surface area). Whereas at high temperature (or longer time), due to the MgO sintering, the rate is determined by the gas-solid reactions independently from the carbon type. Recently, Puig *et al.* [14] proved that a C/MgO molar ratio of 1.25 is sufficient and that biochar carbon gives better yield than carbon black (by around 5%) with a product purity higher than 90%. Moreover, they confirmed that the progressive rise of the temperature, during alumina carbo-reduction at 900 Pa, allows to limit the formation of undesirable by-products as CO emission is spread out over time, and thus to obtain higher yield and metal content [15]. Similar conclusion was obtained during the magnesia reduction, showing that reducing the heating rate improves both the reaction rate and yield [16], [17].

One important parameter during the carbothermal reduction of magnesia is the milling of the C/MgO reactants as the mass loss rises from 24% without milling to 40, 51, 58, and 67% with 1, 2, 4, and

8 h of milling respectively. Increasing the milling time affects the size of MgO particles (decrease from 50 to 15 nm) and the specific surface area of the MgO/C sample (increase from 5 to 110 m^2/g) [18], [19]. Additionally, CaF_2 binder proved to have a catalytic effect during the carbothermal reduction of magnesia at 1723 K under 30-100 Pa, as the reduction rate increases with an optimal quantity of 5% CaF_2 [20]. Moreover, mechanical tests showed that pellets with 5% bentonite / 5% starch binders have the best strength where the bentonite conserves the strength under heat while the starch is decomposed into char, which might be profitable for the later-on reduction process [21].

Herein, we investigated the improvement of the carbothermal reduction of magnesia in the Sol@rmet reactor using concentrated solar energy for the production of metallic Mg powders. This can be achieved by adjusting the circulation of the argon flow (controlling $P_{reactor}$ and P_{CO}), increasing the temperature progressively and adding various binders.

2. Experimental Setup

The carbothermal reduction of magnesia was performed in the Sol@rmet reactor using a 1.5 kW solar furnace that concentrate the solar power up to 11000 suns. The reaction temperature was controlled by opening the shutter placed between the heliostat and the parabolic mirror as shown in **Figure 1**.

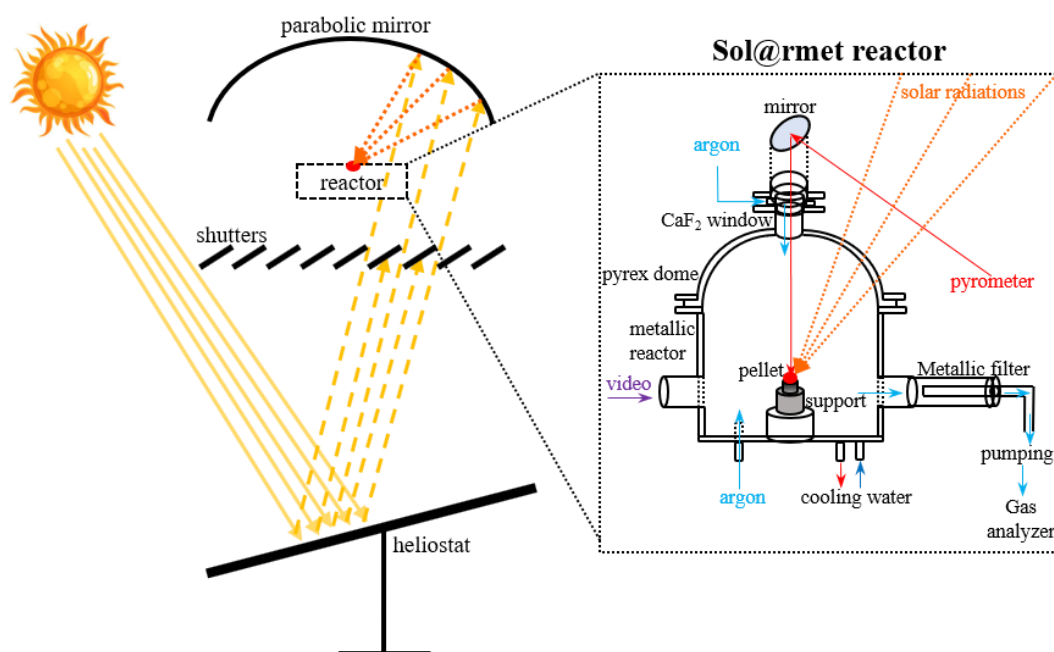


Figure 1. Scheme of the experimental set-up including the concentrating solar system and the Sol@rmet reactor

The Sol@rmet reactor consists of a cooled metallic part and a glass dome allowing the passage of the solar radiation (**Figure 2**). An optical monochromatic (5 μm) pyrometer (Heitronics K15.42 II) was used to measure the temperature of the sample and supposing that the normal spectral emissivity of the sample is 0.95 at this wavelength. However, modelling results showed that the temperature of the pyrometer is 100-200 K higher than the real temperature of the sample surface [14]. Vacuum was applied using a dry primary pump (Edwards nXDS15i) having a maximum pumping rate of 15 m^3/h . The operating pressure inside the reactor was regulated by controlling the argon flow using mass flow controllers. Pure MgO (Sigma-Aldrich, 325 mesh, > 99%) and various carbon reducing agents (birch and starch charcoals, graphite M291, carbon black), with a C/MgO ratio of 1.25, were milled mechanically using Fritsch Pulverisette 4 mill. Various binders as polyvinyl alcohol (PVA), bentonite, and starch (Avedex 36 LAC 14, Avebe) were added with different percentages. Cylindrical pellets ($\varnothing = 8 \text{ mm}$, thickness = 2-3 mm) were then formed by dry pressing powders at one ton.

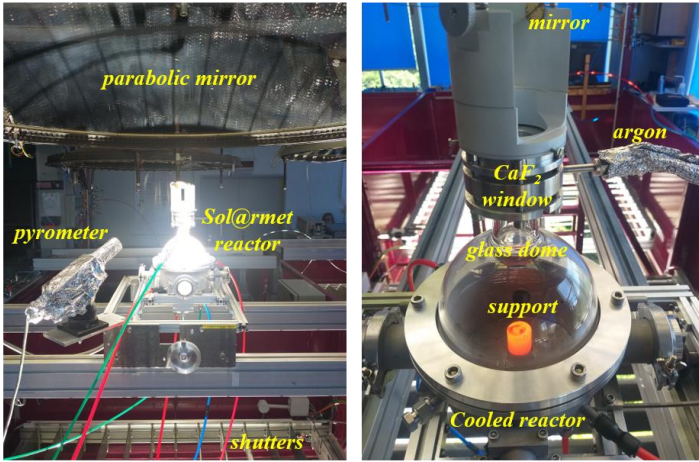


Figure 2. Photos of the Sol@rmet reactor during the reaction (left), and seconds after the end of the reaction (right)

All experiments were performed when the direct normal irradiation (DNI) is of 900-1020 W/m^2 with a change less of 3% during each experiment. The produced powders were collected on a porous stainless-steel filter (98% retention of 0.2 μm particles) placed on the entry of the pumping tube (with a small quantity on the reactor walls), while the

produced CO and CO₂ were analysed during the reaction using the Xstream gas analyser (Emerson). The collected powders were analysed by X-ray diffraction (PANalytical X'Pert Pro) and the percentages of Mg and MgO were quantified using Highscore Plus software (comparing to International Centre for Diffraction Data ICDD files using reference intensity ratio technique).

The performance of the magnesia reduction was determined by computing the magnesium metallic yield (y_{Mg}) according to **Eq. 1**, where m_{Mgmax} is the maximum quantity of Mg that can be produced taking into account the initial molar quantity of MgO. $\% \text{Mg}_{\text{filter}}$ and $\% \text{Mg}_{\text{reactor}}$ are the percentages of Mg in the collected powders on the filter and the reactor walls, respectively. The accuracy of the Mg quantification method was estimated to be lower than 10% for a Mg percentage higher than 90% [14]. Thus, a relative error of about $\pm 5\%$ is considered for the results of the Mg yield.

$$y_{\text{Mg}} (\%) = 100(m_{\text{filter}}\% \text{Mg}_{\text{filter}} + m_{\text{reactor}}\% \text{Mg}_{\text{reactor}})/m_{\text{Mgmax}} \quad (1)$$

3. Results and Discussion

In this section, we present and discuss the results of the solar experiments highlighting the effect of the gas circulation in the Sol@rmet reactor, the advantage of the mechanical milling of the C/MgO powders and the catalytic-like role of the bentonite binder.

3. 1. Effect of circulating argon flow

Preliminary experiments for the carbothermal reduction of magnesia in the Sol@rmet reactor were performed using birch charcoal by increasing the temperature progressively to optimize the process. During these experiments (A1-A9, Table 1), the carrier gas was injected either from the upper part only or from the upper and lower parts of the reactor. For the primary vacuum, the reactor pressure was adjusted to 900-1000 Pa by controlling the argon flow. Results, presented in Table 1, show the importance of creating a swirl circulation flow in the reactor, which prevents the deposition of produced metal powders on the glass dome and allows purging the produced CO from the reactor and thus reducing its partial pressure and accelerating the reaction.

Table 1. Tests for the improvement of the solar carbothermal reduction of magnesia: operating conditions, Mg yield and purity

Test	MgO	m _{pellet} (mg)	observations	T (K)	time (min)	Mg yield* (%)	Purity (%Mg _{filter})
A1	pure	145.3	pure MgO	1610-1800	prog 28 + held 2	32	60
A2	calcined	139.3	calcined MgO	1920-2190	prog 28 + held 7	39	60
A3	calcined	141.5	+ PVA binder	1790-2170	prog 28 + held 5	48	82
A4	calcined	139.4	lower reaction time	1920-2230	prog 15 + held 9	52	87
A5	calcined	138.7	non-controllable upper/lower flow	1930-2100	prog 15 + held 9	67	84
A6	calcined	139.7	90%Ar-10%CO flow	1940-2090	prog 16 + held 9	29	87
A7	pure	137.2	controllable upper/lower flow	2160-2290	prog 15 + held 5	54	92
A8	pure	139.7	use of metallic filter	1970-2130	prog 15 + held 2	68	87
A9	pure	397.8	higher pellet mass	1780-2550	prog 26 + held 3	69	95

*The magnesium yield percentage accounts the powders collected on the filter and the reactor walls (see Eq. 1).

Comparing tests A1 and A2 proved that the calcination of MgO reactant (at 1273 K for 3 h) improves the reaction yield. Furthermore, adding PVA binder, as in test A3, increases the metallic yield by around 10%. However, it appears from test A4 (no binder) that lowering the reaction time, and thus increasing the pellet temperature, gives a yield of 52% suppressing the beneficial effect of PVA. During all previous tests (A1-A4), the main problem is the deposition of the produced magnesium on the reactor walls and glass dome. Thus, in the following tests (A5-A9), argon is injected from both the upper and lower parts of the reactor, which creates a swirl flow inside the reactor and improves the reduction. This is observed in test A5, where using a non-controllable upper and lower argon flow allows to achieve a total yield of 67%. The textural properties of the produced powders, collected on the filter, after test A5, are determined by scanning electron microscopy (SEM) and the corresponding images (Figure 3) showed that 10-100 μm agglomerates of micron and submicron grains were obtained.

Changing the carrier gas into 90%Ar-10%CO, in test A6, decreases the yield to around 30%, thus it is not advantageous to use 10%CO as it promotes the reverse reaction. During test A7, pure MgO is used to reduce the steps of the process. The argon flow is injected from the upper and lower parts of the reactor at 0.5 and 3 L/min respectively. High temperatures, up to 2300 K, are reached giving 54% Mg yield (92% Mg purity on the filter). However, this value is much lower than the one obtained in test A5 using calcined MgO. In test A8, the ceramic filter is replaced by a

metallic filter, which improves the collection of the metallic products and increases the yield to 68%. Increasing the pellet mass, in test A9, is advantageous giving highly pure Mg powders (95%) with the maximal yield of 69% and temperatures attaining 2550 K.

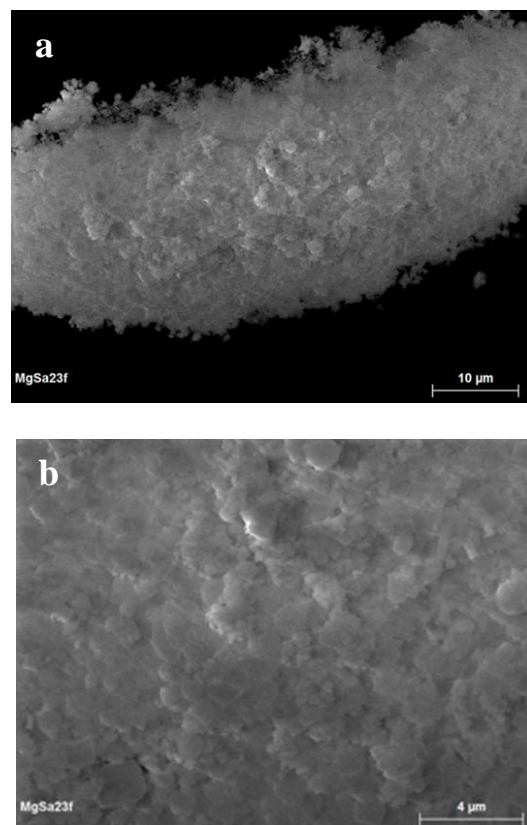


Figure 3. Scanning electron microscopy images of the produced Mg agglomerates (a) of submicron particles (b) collected on the filter after test A5

3.2. Effect of the reducing agent

The following experiments were performed to compare the effect of the various carbon reducing agents as birch and starch charcoals, graphite M291 and carbon black. Based on the previous section, a double argon flow, of 1 and 3.5 L/min from the upper and lower parts of the reactor respectively, is used giving an operating pressure of 840 Pa. The temperature was increased progressively by opening the shutter each two minutes as shown in Figure 4. The reaction was ended after 18 min by closing the shutter without considering if the reaction is still going or not. Figure 4 shows the progress of the reaction with time for the different carbon reducing agents by comparing the CO emission and the temperature. We can observe that the temperature was similar when using birch charcoal or carbon black (around 2250 K), while the CO emission was much higher using birch charcoal compared to when using carbon black (about 6000 ppm compared to 2000 ppm at 50% shutter opening). This indicates

that the reduction is affected by the carbon structure and the C/MgO contact, not only from the reaction temperature.

Results showed that both birch (wood-based) and starch (vegetable-based) charcoals allowed to reach a Mg yield, of about 60%, much higher than that obtained when using graphite M291 (38% Mg yield) or carbon black (30% Mg yield). Those results were obtained despite that graphite has a similar fixed carbon content as birch charcoal (94% C) and a higher specific surface area (250 compared to 150 m²/g). This can be attributed to the highly-active amorphous structure of charcoals compared to the crystalline structure of graphite and carbon black [22]. Those findings were consistent with previous studies showing that charcoal outperforms graphite [12] and carbon black [13] when operating under vacuum conditions and when the C/MgO solid-solid reaction dominates [14]. For all types of the reducing agent, the powders were highly pure (> 95% Mg).

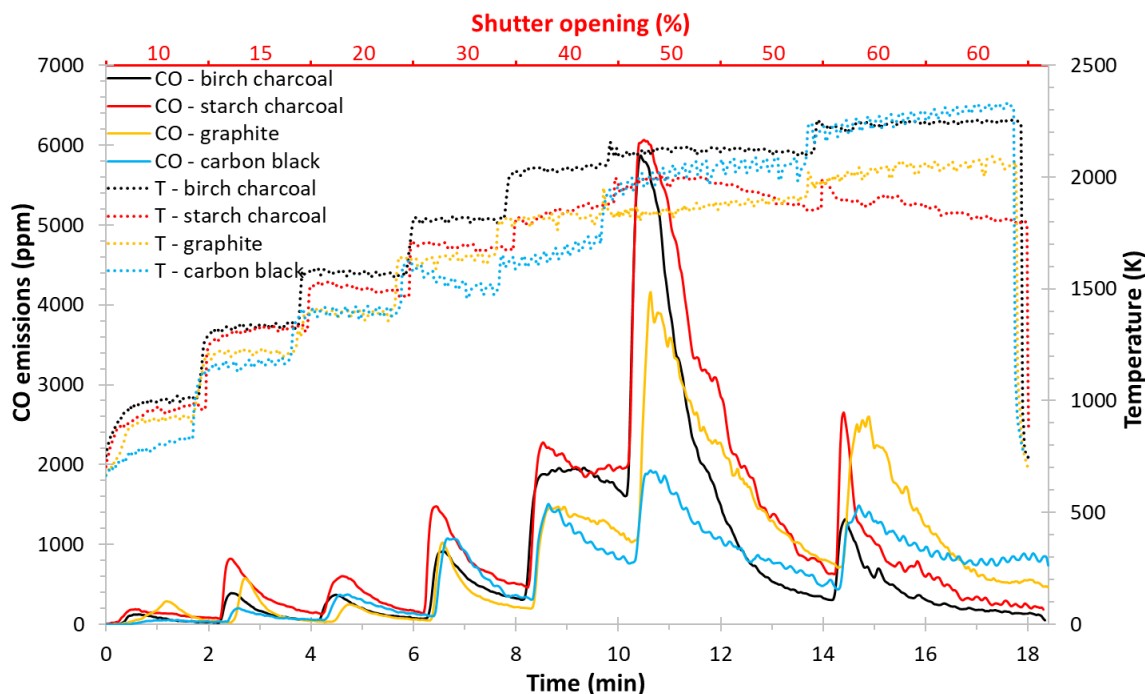


Figure 4. Reaction progress through temperature and CO emission profiles during the carbothermal reduction of magnesia using different reducing agents

3.3. Effect of milling and binders

The following experiments (B1-B6) were performed using birch charcoal and a double argon flow (1 and 3.5 L/min, 840 Pa). They are performed by increasing the temperature progressively (opening

the shutter) each two minutes, and the reaction is ended when the CO production becomes lower than 200 ppm (around 2-3 min). Thus, the total time of the reaction is around 22-23 min. **Table 2** presents the conditions (temperature and DNI) and gas emissions

(CO and CO₂) progress with time during the reduction of the C/MgO + 10% PVA pellet (test B1).

Table 2. Parameters progress with time during the reduction of the C/MgO + 10% PVA pellet (test B1): conditions (T and DNI) and gas production (CO and CO₂)

t (min)	Shutter opening (%)	DNI (W/m ²)	T (K)	CO peak (ppm)	CO ₂ peak (ppm)
0	10	917	940	28	228
2	15	919	1300	434	142
4	20	919	1520	376	37
6	30	922	1800	911	*
8	40	922	2020	1942	*
10	50	925	2130	6426	*
12	60	925	2250	3784	*
14	70	926	2340	2105	*
16	80	929	2480	1468	*
18	90	927	2530	407	*
20	100	929	2570	405	*
22	100	929	2560	180	*

The temperature profile during the reduction of the C/MgO + 10% PVA pellet (test B1) is illustrated as a function of the reaction time and shutter opening in Figure 5. The collected powders (on the filter or in the reactor) are analysed by XRD and quantified to determine their purities. The XRD pattern of the powders collected on the filter after the reduction of the C/MgO + 10% PVA pellet is presented in Figure 6, where only Mg and MgO peaks are detected and quantified.

The performance of various C/MgO pellets, depending on the binder type (PVA, starch, and/or bentonite), is examined and compared in Table 3. When using 10% PVA (test B1), most of the products is collected on the metallic filter with 93% purity and a total Mg yield (filter + reactor) of 83%. This value is much better than those obtained during the preliminary experiments (tests A1-A9) in the first section where a maximum of 69% is reached. This difference highlights the effect of the mechanical milling of the carbon and magnesia particles together before forming the pellets. This could be attributed to the decrease of the size of the C and MgO particles and the increase of the C/MgO surface contact, thus accelerating the phase boundary reaction that proved to be the rate-controlling step during the high temperature reduction.

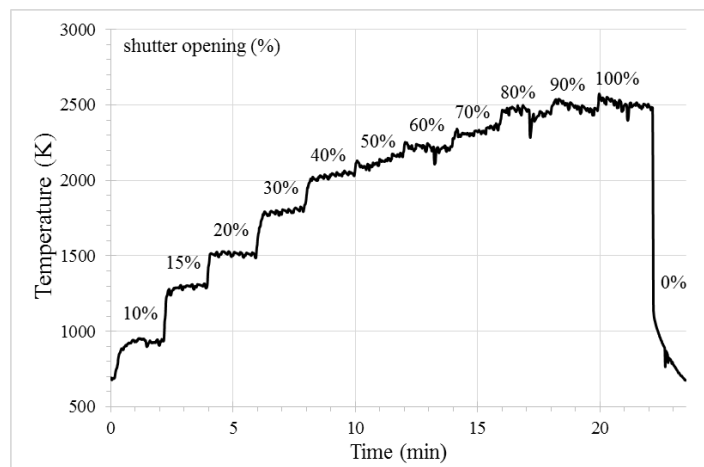


Figure 5. Temperature profile as a function of time and shutter opening during the reduction of C/MgO + 10% PVA pellet (test B1)

When using 5% starch + 5% bentonite as binders (tests B2 and B3), a metal yield up to 96% with 96% Mg purity is achieved with only 5 mg of the pellet remains. The difference between the two tests can be attributed to the DNI (B2: 951-962 W/m² and B3: 998-1004 W/m²), as the temperature at 15% shutter opening during B2 is of 1250 K compared to 1300 K during B3.

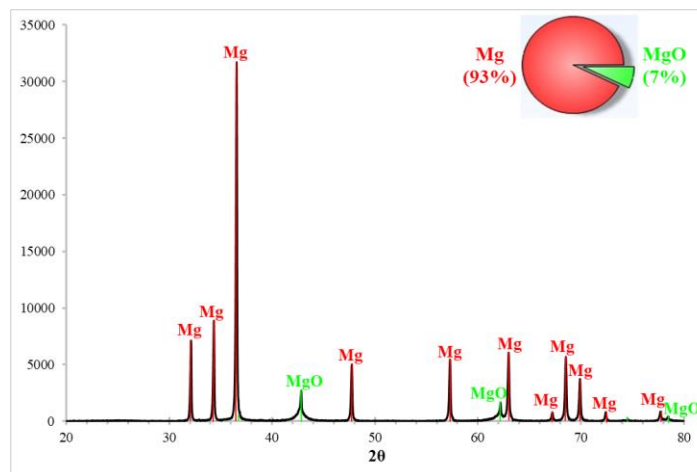


Figure 6. XRD pattern of the powders collected from the filter after the reduction of the C/MgO + 10% PVA pellet (test B1)

When the pellet mass is reduced to 200 mg (test B4), the reaction yield decreases slightly to around 91%, which is consistent with previous results (comparing tests A8 and A9) proving that increasing the pellet mass will improve the reduction rate.

During tests B5 and B6, starch is used as a binder with 10% and 5% respectively, giving yields of about 76-77% with a smaller preference when less binder is used. Thus, comparing all experiments proved that PVA and bentonite binders act as catalysts for the carbothermal reduction of magnesia. Around 12 mg of

the pellet did not react during test B6, and were characterized by XRD proving that the remaining part consists of a mix of magnesia (54%), magnesium carbonate $Mg(CO_3)$ (around 29%), and carbon (17% including 9% graphite).

Table 3. Performance of various pellets depending on the binder type during the carbothermal reduction of magnesia

Test	binder	m_{pellet} (mg)	T_{max} (K)	m_{remain} (mg)	m_{filter} (mg)	% Mg_{filter}^*	m_{reactor} (mg)	% Mg_{reactor}^*	Mg yield (%)
B1	10% PVA	252	2570	21.1	82.7	93	10.1	83	84.7
B2	5% starch + 5% bentonite	248	2480	10.1	77.3	96	21.4	58	87.4
B3	5% starch + 5% bentonite	248	2480	5	85.7	96	21.8	58	95.8
B4	5% starch + 5% bentonite	208	2390	4.2	69.1	96	15.4	58	90.6
B5	10% starch	250	2540	17.4	74.7	93	9	74	76.2
B6	5% starch	253	2600	12	79.6	93	10.7	74	77.4

*XRD analysis are performed for tests B1, B3 (same value admitted for B2 and B4), and B6 (same value for B5).

5. Conclusion

The advantageous properties of the metallic powders when used as transportation fuels make it necessarily to develop new sustainable processes for their production. Hence, we investigated the improvement of the vacuum-assisted carbothermal reduction of magnesia in the Sol@rmet reactor using concentrated solar energy and charcoal reducing agent as renewable sources. Experiments proved that creating a good circulating swirl flow of the carrier gas inside the reactor, through the injection from the upper and lower parts of the reactor, would reduce the CO partial pressure through its purging and thus accelerating the reaction rate. Moreover, increasing the reaction temperature progressively over a reduced retention time allows achieving higher temperatures and thus higher reduction yields. Further, using a metallic filter improves the collection of the produced magnesium powders. Furthermore, birch and starch charcoals as reducing agents allowed to reach a higher Mg yield than when using graphite or carbon black. Finally, results showed that PVA and bentonite binders have a catalytic effect during the reaction with a highest Mg yield value, of 96% with 96% Mg purity, reached using a C/MgO molar ratio of 1.25 with 5% starch + 5% bentonite binder (maximal temperature around 2500 K). However, despite that higher temperatures (up to 2600 K) are reached

when using 5% starch, lower Mg yield is obtained (77%).

Acknowledgments

This study is funded through the STELLAR project by the French National Research Agency (ANR) under contract ANR-18-CE05-0040-02. This work is supported by the French “Investments for the future” program managed by the ANR under contract ANR-10-EQPX-49-SOCRATE (Equipex SOCRATE).

References

- [1] M. Höök and X. Tang, “Depletion of fossil fuels and anthropogenic climate change—A review,” *Energy Policy*, vol. 52, pp. 797–809, 2013, doi: 10.1016/j.enpol.2012.10.046.
- [2] J. M. Bergthorson, S. Goroshin, M. J. Soo, P. Julien, J. Palecka, D. L. Frost, and D. J. Jarvis, “Direct combustion of recyclable metal fuels for zero-carbon heat and power,” *Applied Energy*, vol. 160, pp. 368–382, 2015, doi: 10.1016/j.apenergy.2015.09.037.
- [3] A. Steinfeld, P. Kuhn, and Y. Tamaura, “ CH_4 -utilization and CO_2 -mitigation in the metallurgical industry via solar thermochemistry,” *Energy Conversion and Management*, vol. 37, no. 6–8, pp. 1327–1332, 1996, doi: 10.1016/0196-8904(95)00341-X.

- [4] A. Steinfeld and R. Palumbo, "Solar Thermochemical Process Technology," in *Encyclopedia of Physical Science and Technology*, Elsevier, 2003, pp. 237–256. doi: 10.1016/B0-12-227410-5/00698-0.
- [5] E. Balomenos, D. Panias, and I. Paspaliaris, "Exergy Analysis of Metal Oxide Carbothermic Reduction under Vacuum – Sustainability prospects," *Int. J. Thermo*, vol. 15, no. 3, pp. 141–148, 2012, doi: 10.5541/ijot.376.
- [6] J. Puig and M. Balat-Pichelin, "Production of metallic nanopowders (Mg, Al) by solar carbothermal reduction of their oxides at low pressure," *Journal of Magnesium and Alloys*, vol. 4, no. 2, pp. 140–150, 2016, doi: 10.1016/j.jma.2016.05.003.
- [7] N. Xiong, Y. Tian, B. Yang, B. Xu, T. Dai, and Y. Dai, "Results of recent investigations of magnesia carbothermal reduction in vacuum," *Vacuum*, vol. 160, pp. 213–225, 2019, doi: 10.1016/j.vacuum.2018.11.007.
- [8] I. Hischier, B. A. Chubukov, M. A. Wallace, R. P. Fisher, A. W. Palumbo, S. C. Rowe, A. J. Groehn, and A. W. Weimer, "A novel experimental method to study metal vapor condensation/oxidation: Mg in CO and CO₂ at reduced pressures," *Solar Energy*, vol. 139, pp. 389–397, 2016, doi: 10.1016/j.solener.2016.10.024.
- [9] I. Vishnevetsky and M. Epstein, "Solar carbothermic reduction of alumina, magnesia and boria under vacuum," *Solar Energy*, vol. 111, pp. 236–251, 2015, doi: 10.1016/j.solener.2014.10.039.
- [10] I. Vishnevetsky, "Solar Thermal Reduction of Metal Oxides as a Promising Way of Converting CSP Into Clean Electricity on Demand," in *Proceedings of the ISES Solar World Congress 2015*, Daegu, Korea, 2016, pp. 1–12. doi: 10.18086/swc.2015.04.23.
- [11] R. J. Fruehan and L. J. Martonik, "The Rate of reduction of MgO by carbon," *MTB*, vol. 7, no. 4, pp. 537–542, 1976, doi: 10.1007/BF02698585.
- [12] L. Rongti, P. Wei, M. Sano, and J. Li, "Kinetics of reduction of magnesia with carbon," *Thermochimica Acta*, vol. 390, no. 1–2, pp. 145–151, 2002, doi: 10.1016/S0040-6031(02)00128-4.
- [13] G. Levêque and S. Abanades, "Investigation of thermal and carbothermal reduction of volatile oxides (ZnO, SnO₂, GeO₂, and MgO) via solar-driven vacuum thermogravimetry for thermochemical production of solar fuels," *Thermochimica Acta*, vol. 605, pp. 86–94, 2015, doi: 10.1016/j.tca.2015.02.015.
- [14] J. Puig and M. Balat-Pichelin, "Experimental carbothermal reduction of MgO at low pressure using concentrated solar energy," *J min metall B Metall*, vol. 54, no. 1, pp. 39–50, 2018, doi: 10.2298/JMMB170215048P.
- [15] J. Puig, M. Balat-Pichelin, and E. Beche, "Solar metallurgy for the production of Al and Mg particles," in *SolarPACES 2017*, Santiago, Chile, 2018, vol. 2033, p. 140002. doi: 10.1063/1.5067153.
- [16] L. Rongti, P. Wei, and M. Sano, "Kinetics and mechanism of carbothermic reduction of magnesia," *Metall and Materi Trans B*, vol. 34, no. 4, pp. 433–437, 2003, doi: 10.1007/s11663-003-0069-y.
- [17] L. Rongti, P. Wei, M. Sano, and J. Li, "Catalytic reduction of magnesia by carbon," *Thermochimica Acta*, vol. 398, no. 1–2, pp. 265–267, 2003, doi: 10.1016/S0040-6031(02)00324-6.
- [18] M. Nusheh, H. Yoozbashizadeh, M. Askari, N. Kuwata, J. Kawamura, J. Kano, F. Saito, H. Kobatake, and H. Fukuyama, "Effect of Mechanical Milling on Carbothermic Reduction of Magnesia," *ISIJ Int.*, vol. 50, no. 5, pp. 668–672, 2010, doi: 10.2355/isijinternational.50.668.
- [19] B. A. Chubukov, A. W. Palumbo, S. C. Rowe, M. A. Wallace, and A. W. Weimer, "Enhancing the Rate of Magnesium Oxide Carbothermal Reduction by Catalysis, Milling, and Vacuum Operation," *Ind. Eng. Chem. Res.*, vol. 56, no. 46, pp. 13602–13609, 2017, doi: 10.1021/acs.iecr.7b03175.
- [20] Y. Tian, T. Qu, B. Yang, Y.-N. Dai, B.-Q. Xu, and S. Geng, "Behavior Analysis of CaF₂ in Magnesia Carbothermic Reduction Process in Vacuum," *Metall and Materi Trans B*, vol. 43, no. 3, pp. 657–661, 2012, doi: 10.1007/s11663-011-9622-2.
- [21] B. A. Chubukov, A. W. Palumbo, S. C. Rowe, M. A. Wallace, K. Y. Sun, and A. W. Weimer, "Design and Fabrication of Pellets for Magnesium Production by Carbothermal Reduction," *Metall and Materi Trans B*, vol. 49, no. 5, pp. 2209–2218, 2018, doi: 10.1007/s11663-018-1309-5.
- [22] Y. Jiang, H. W. Ma, and Y. Q. Liu, "Experimental Study on Carbothermic Reduction of Magnesia with Different Carbon Materials," *AMR*, vol. 652–654, pp. 2552–2555, 2013, doi: 10.4028/www.scientific.net/AMR.652-654.2552.